Nuclear temperatures from evaporation fragment spectra and observed anomalies

A. Ray,[1,*] A. De,[2] A. Chatterjee,[3] S. Kailas,[3] S. R. Banerjee,[1] K. Banerjee,[1] and S. Saha[4]

[1]*Variable Energy Cyclotron Center, 1/AF, Bidhannagar, Kolkata 700064, India*

[2]*Raniganj Girls' College, Raniganj, Bardhaman 713358, West Bengal, India*

[3]*Nuclear Physics Division, Bhabha Atomic Research Center, Mumbai 400085, India*

[4]*Saha Institute of Nuclear Physics, 1/AF, Bidhannagar, Kolkata 700064, India*

(Received 5 February 2013; revised manuscript received 2 May 2013; published 10 June 2013)

The extreme back-angle evaporation spectra of alpha, lithium, beryllium, boron and carbon from different compound nuclei near $A \approx 100$ ($E_X = 76$–210 MeV) have been compared with the predictions of standard statistical model codes such as CASCADE and GEMINI. It was found that the shapes of the alpha spectra agree well with the predictions of the statistical models. However, the spectra of lithium, beryllium, boron, and carbon show significantly gentler slopes implying higher temperature of the residual nuclei, even though the spectra satisfy all other empirical criteria of statistical emissions. The observed slope anomaly was found to be largest for lithium and decreases at higher excitation energy. These results could not be understood by adjusting the parameters of the statistical models or from reaction dynamics and might require examining the statistical model from a quantum mechanical perspective.

DOI: 10.1103/PhysRevC.87.064604 PACS number(s): 25.70.Gh, 25.70.Jj

I. INTRODUCTION

The temperature of a system is defined when it is in thermal statistical equilibrium with, in principle, infinite lifetime. The atomic nucleus is a microscopic system and the temperature of a nucleus is determined from the emission of the small parts of the nucleus itself, assuming the formation of long-lived unstable dinuclear states of the fragment and the residual nuclei in the exit channel and the statistical decay of those states. Generally, the temperature of the residual nucleus is determined from the slope of the evaporation neutron, proton or alpha spectra. Charity *et al.* [1] studied extensively the spectral shapes of the evaporation neutron, proton and alpha particles from a large number of compound nuclei and fitted them using the statistical model code GEMINI. They [1] needed an excitation energy dependent level-density parameter to explain the spectral shapes of the evaporation neutron, proton and alpha spectra from the heavier compound nuclei ($A > 150$). However, in order to understand the evaporation spectra from the lighter compound nuclei ($A \leqslant 100$), no such excitation energy dependent level-density parameter was required [1].

So far, there has not been any significant effort to understand the spectral shapes of heavier evaporation fragments such as lithium, beryllium, boron and carbon by comparing them with the standard statistical model codes. The absolute cross sections of such fragments as calculated from the statistical model codes are rather sensitive to many parameters of the statistical model such as the transmission coefficients, critical angular momentum, diffusivity of the spin distribution and the level-density parameter. On the other hand, the spectral shape is largely insensitive to most of those parameters except the level-density parameter. In the case of compound nuclei in the $A \approx 100$ mass region, level-density parameter becomes almost independent of the excitation energy as found by Charity *et al.* [1]. So it would be somewhat simpler to study and compare the evaporation fragment spectra from the compound nuclei in the $A \approx 100$ mass region with the statistical model codes. In this paper, we have compared the extreme back-angle evaporation spectra of alpha, lithium, beryllium, boron and carbon particles from $^{16}O + {}^{89}Y$, $^{16}O + {}^{93}Nb$ and $^{3}He + Ag$ reactions producing the compound nuclei in the $A \approx 100$ mass region (having excitation energies ranging from $E_X = 76$ to 210 MeV) with the statistical model codes CASCADE [2] and GEMINI [1]. The statistical character of the spectra has been demonstrated from the observed back-angle rise of the angular distribution and lack of any entrance-channel dependence of the spectra for $^{16}O + {}^{89}Y$ and $^{12}C + {}^{93}Nb$ reactions forming the same compound nucleus with similar spin distribution and excitation energy. In the case of the $^{3}He + Ag$ reaction, the data were taken from Refs. [3,4] and the authors concluded from their detailed analysis that the back-angle heavy-ion spectra should be statistical. It has been found from our comparison that the observed spectral shapes of the alpha particles agree well with the statistical model calculations, but the experimental spectra of the heavier fragments (particularly lithium, beryllium and boron) show significantly gentler slope (than the statistical model calculations) implying higher-than-expected temperature of the residual nuclei for ^{16}O, ^{12}C, and ^{3}He induced reactions. In Sec. II, we discuss statistical model calculations and compare between the calculated spectra from CASCADE and GEMINI codes. The analysis of the experimental results is presented in Sec. III. Discussions of the results are presented in Sec. IV. Finally the conclusion is given in Sec. V.

II. STATISTICAL MODEL PREDICTIONS

One of the standard methods of the measurement of the temperature of the ensemble of residual nuclei (at the instant of the breakup of the exit-channel dinuclear system comprising residual and the emitted fragment) is by measuring the slope of the exponential tail of the spectrum of the emitted particles, provided the decay is statistical. The statistical evaporation

*ray@vecc.gov.in

spectrum of fragments emitted from a compound nucleus can be written [5,6] as

$$P(x) \propto \exp\left(-\frac{x}{T}\right) \operatorname{erfc}\left(\frac{p-2x}{2\sqrt{pT}}\right), \quad x = E_{\rm kin}\,({\rm c.m.}) - V_C. \tag{1}$$

Here $E_{\rm kin}$ (c.m.), p, T, and $P(x)$ are the exit-channel center-of-mass kinetic energy, amplification parameter, temperature of the ensemble of the residual nuclei, and the corresponding probability of the emission of the particle, respectively. V_C is a parameter that is equal to the Coulomb barrier for the zero orbital angular momentum of the system [5]. Usually for low-energy nuclear reactions, the temperature is obtained by fitting evaporation proton and alpha spectra from an ensemble of compound nuclei with Eq. (1) [6,7]. It was found [6,7] that high-statistics alpha spectra can be fitted within a few percent using a one-source term as given in Eq. (1) and that an average temperature of the ensemble of the residual nuclei can be extracted. The effect of the sequential decay can be considered by adding up several source terms [such as Eq. (1)] with decreasing temperatures [8]. The inclusion of additional two- or three-source terms with decreasing temperatures can fit experimental spectra within 0.5% [8]. It should be possible to use the heavier fragment (such as Li, Be, B, C) evaporation spectra to determine the temperatures of the corresponding ensembles of the residual nuclei, provided those emissions are statistical. At relatively lower excitation energy when the orbital kinetic energies taken away by the heavier fragments remain significant compared to the excitation energy of the compound system, the temperatures of the residual nuclei obtained by fitting heavier fragment evaporation spectra are generally expected to be lower compared to those obtained from proton or alpha spectra.

We used the statistical model code CASCADE [2] to calculate the spectra of the neutron, proton, alpha and heavier fragments from the ^{16}O + ^{89}Y reaction at $E_{\rm Lab}(^{16}{\rm O}) = 96$ MeV. In the CASCADE code, the neutron, proton and alpha particles were the main particle emission channels and the lithium or boron or carbon particle was used as a fourth particle channel one at a time. The CASCADE code executed typically 35 sequential decay steps until the cross section of the evaporation residues fell below 1 mb. The final summed evaporation spectra of the alpha, lithium, beryllium, boron and carbon particles obtained from the calculations were fitted with Eq. (1) to obtain the corresponding slope temperatures which should indicate the average temperatures of the corresponding ensembles of the residual nuclei. The GEMINI code [1] calculations were done to compare with the CASCADE code calculations. In the GEMINI code, neutron, proton, alpha, and lithium particle emissions were calculated using the Hauser-Feshback transition state formalism. The emissions of heavier fragments such as beryllium, boron and carbon were treated as evaporation emissions simultaneously. The emission of the fragments from the sequential decay of the prefragments (those are produced in the initial binary decay of the compound nucleus) is included in the GEMINI code. The GEMINI code gave relative cross sections for the emission of different ions and the spectra were normalized with respect to the corresponding

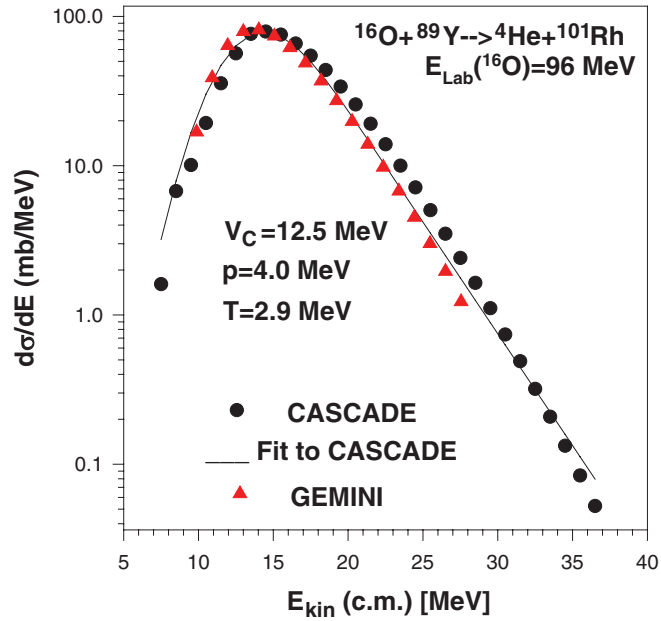

FIG. 1. (Color online) Statistical model CASCADE and GEMINI code calculations of the ^{4}He spectrum from the ^{16}O + ^{89}Y reaction at $E_{\rm Lab}(^{16}{\rm O}) = 96$ MeV and the corresponding fit (smooth line) using Eq. (1). The GEMINI code calculations have been normalized to match with the CASCADE code calculations.

calculated spectra from the CASCADE code to compare the corresponding spectral shapes calculated from the two codes. The calculated spectral shapes of alpha, lithium, beryllium, boron and carbon obtained from the CASCADE agree very well with the corresponding spectral shapes calculated by the GEMINI code. In Fig. 1, we show the calculated alpha spectra (in the center-of-mass frame) for both the CASCADE and GEMINI codes and a fit using Eq. (1). The fit yields $T = 2.9$ MeV, $p = 4.0$ MeV and $V_C = 12.5$ MeV. In Figs. 2–5, we show the calculated ^{6}Li, ^{9}Be, ^{11}B and ^{12}C spectra using the CASCADE and GEMINI codes and fits to corresponding CASCADE calculations using Eq. (1). In the case of calculating carbon emission using CASCADE code (Fig. 5), the liquid drop moment of inertia was multiplied by 0.9 to match with the slope of the corresponding GEMINI spectrum. The results of the fits have been presented in Table I. It was found that the temperatures of the residual nuclei generally decrease for the emission of the heavier fragments as expected at such low excitation energy ($E_X = 76$ MeV). On the other hand, the value of the amplification parameter (p) increases from 4.0 MeV for the alpha particle to 20.0 MeV for the carbon particle.

The calculations have been done using the level-density parameter $a = A/8$ and the extracted parameters (T and p) are essentially independent of the transmission coefficients, deformation parameter, critical angular momentum, etc. used in the calculations. The use of different optical-model parameters resulting in a different set of transmission coefficients and different critical angular momenta change the calculated cross sections of the heavy fragments considerably, but hardly affect the slope of the exponential tail of the spectrum and the corresponding extracted temperature, because the distribution

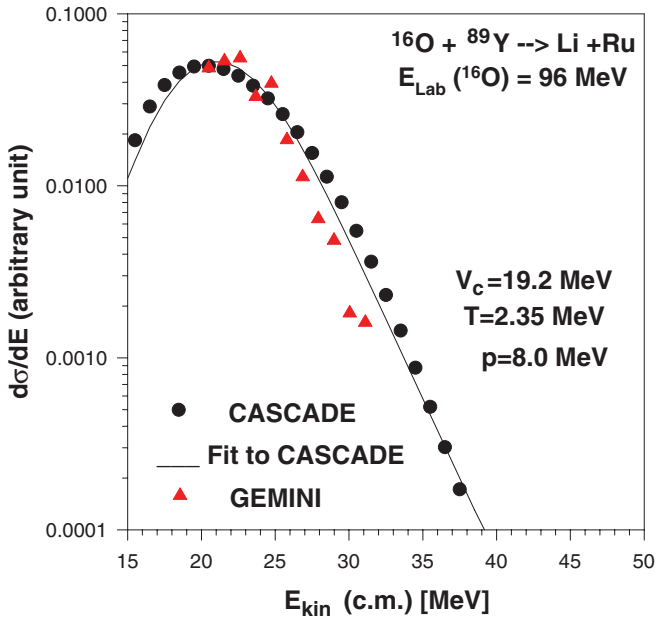

FIG. 2. (Color online) Statistical model CASCADE and GEMINI code calculations of the lithium spectrum from the ^{16}O + ^{89}Y reaction at $E_{Lab}(^{16}O) = 96$ MeV and the corresponding fit (smooth line) using Eq. (1). The GEMINI calculations have been normalized to match with the CASCADE calculations.

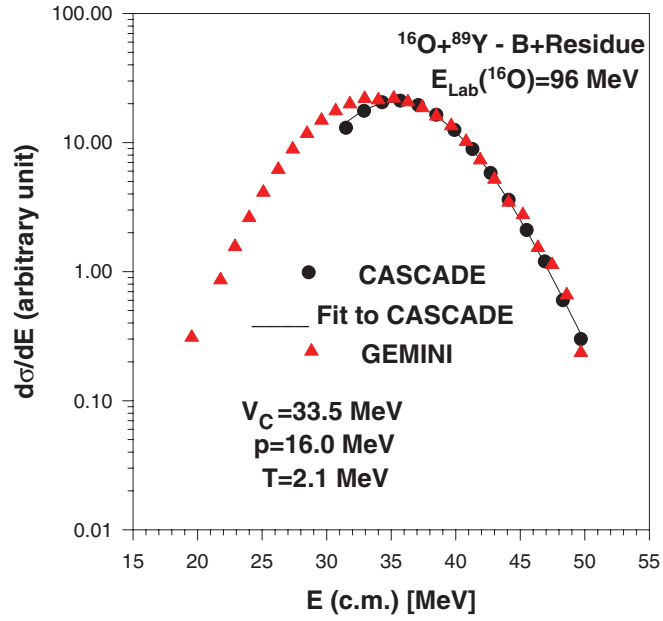

FIG. 4. (Color online) Statistical model CASCADE and GEMINI code calculations of the boron spectrum from the ^{16}O + ^{89}Y reaction at $E_{Lab}(^{16}O) = 96$ MeV and the corresponding fit (smooth line) using Eq. (1). The GEMINI calculations have been normalized to match with the CASCADE calculations.

of the excitation energy of the residual nuclei essentially remains independent of the transmission coefficients of the ejectiles. So we have normalized the calculated statistical-model spectra of heavy ions (Li, Be, B, C) with respect to the experimental spectra and compared the corresponding spectral shapes. The statistical model calculations have also been done considering the emission of heavy ions in their first and second excited states and the corresponding spectral shapes remain essentially unchanged. The qualitative features of the calculations showing substantial lower temperature from the heavy fragment spectra is model independent and essentially

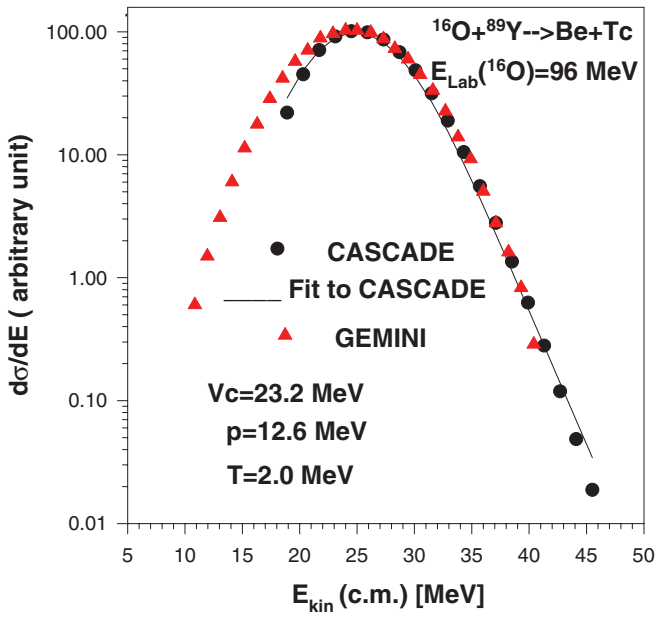

FIG. 3. (Color online) Statistical model CASCADE and GEMINI code calculations of the beryllium spectrum from the ^{16}O + ^{89}Y reaction at $E_{Lab}(^{16}O) = 96$ MeV and the corresponding fit (smooth line) using Eq. (1). The GEMINI calculations have been normalized to match with the CASCADE calculations.

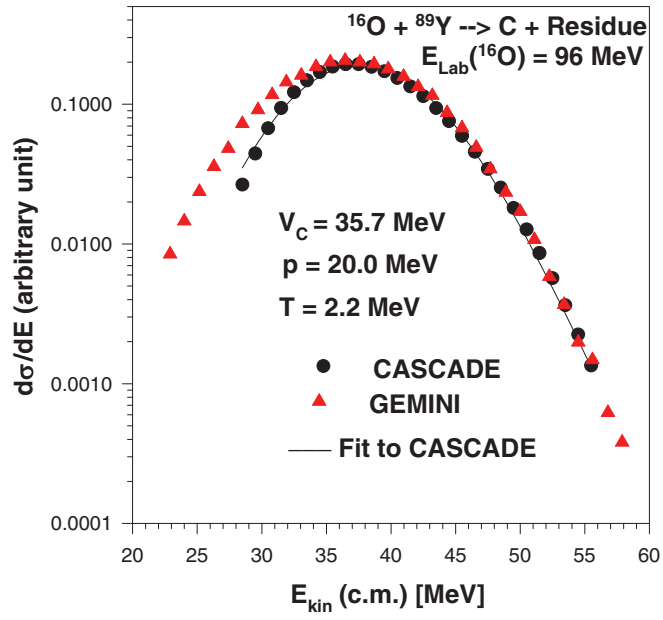

FIG. 5. (Color online) Statistical model CASCADE and GEMINI code calculations of the carbon spectrum from the ^{16}O + ^{89}Y reaction at $E_{Lab}(^{16}O) = 96$ MeV and the corresponding fit (smooth line) using Eq. (1). The GEMINI calculations have been normalized to match with the CASCADE calculations.

follows from the fact that the heavy fragments take away a significant fraction of the available energy as their kinetic energies, and also because the masses of the residual nuclei are not significantly lower than the mass of the parent compound nucleus.

The CASCADE code [2] calculations were done for the ^{3}He + Ag reaction at $E_{\rm Lab}(^3{\rm He}) = 90$ MeV and ^{4}He, ^{6}Li, ^{9}Be, ^{11}B and ^{12}C evaporation spectra were generated. The GEMINI code [1] calculations were also done for the reaction and the evaporation spectra were calculated. The spectral shapes of the evaporation particles obtained from the GEMINI code agree very well with the corresponding spectra obtained from the CASCADE code calculations. In Fig. 6, we show the calculated alpha spectra (in the center-of-mass frame) for both the CASCADE and GEMINI codes and a fit to CASCADE calculation using Eq. (1). The fit yields $T = 3.0$ MeV, $p = 2.0$ MeV and $V_C = 13.5$ MeV. In Figs. 7–9, we show the calculated ^{6}Li, ^{11}B and ^{12}C spectra using the CASCADE and GEMINI codes and fits using Eq. (1). As before, the spectra obtained from the GEMINI code have been normalized to overlay with the spectra obtained from the CASCADE code. The results of the fits have been presented in Table I. It was found that the temperatures of the residual nuclei drop continuously for the emission of the heavier fragments as expected at this low excitation energy ($E_X = 102$ MeV). On the other hand, the value of the amplification parameter (p) increases from 2.0 MeV for the alpha particle to 8.5 MeV for the carbon particle. The calculations have been done using the level-density parameter $a = A/8$ and the extracted parameters are essentially independent of the transmission coefficients used in the calculations. The statistical model (CASCADE and GEMINI) calculations were also performed for the ^{3}He + Ag reaction at $E_{\rm Lab}(^3{\rm He}) = 198.6$ MeV. The temperatures obtained from the calculated ^{4}He, ^{6}Li, ^{9}Be, ^{11}B and ^{12}C spectra have been found to be about the same in all cases ($\approx$4 MeV). This is because the kinetic energies carried away by the heavy fragments are small compared to the excitation energy of the compound nucleus ($E_X = 212$ MeV) and so the extracted temperatures from alpha and heavy ion fragments are about the same. The statistical model calculations were also performed for the ^{16}O + ^{93}Nb reaction at $E_{\rm Lab}(^{16}{\rm O}) = 116$ MeV and the evaporation spectra of alpha, lithium, beryllium, boron, and carbon were generated using the statistical model codes CASCADE and GEMINI. The calculated spectra were fitted with Eq. (1) and the extracted temperature (T) and p parameters have been presented in Table I. According to the GEMINI code, most of the lithium fragments come from the sequential decay of the excited pre-fragments such as beryllium and boron, whereas CASCADE code only calculates the evaporation lithium spectrum. We find that the slope parameters (T) extracted from the lithium spectra calculated by the code GEMINI are similar to those extracted from the corresponding calculated evaporation lithium spectra using the CASCADE code.

III. ANALYSIS OF EXPERIMENTAL DATA

In order to test these predictions, we used both the literature data [3,4] and data from our own experiments. We performed experiments forming [9] the same compound nucleus ^{105}Ag at the same excitation energy ($E_X = 76$ MeV) and with very similar spin distributions ($\ell_{\rm crit}$ equal within 10%) by the ^{16}O + ^{89}Y reaction at $E_{\rm Lab}(^{16}{\rm O}) = 96$ MeV and the ^{12}C + ^{93}Nb reaction at $E_{\rm Lab}(^{12}{\rm C}) = 85.5$ MeV. The details

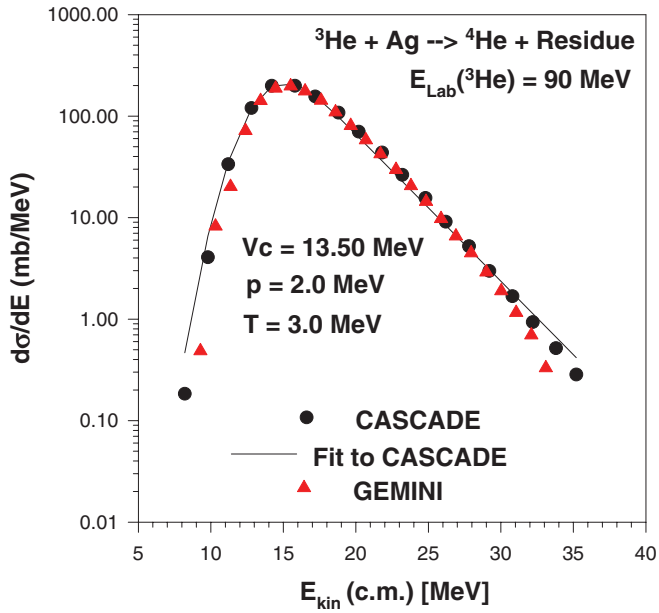

FIG. 6. (Color online) Statistical model CASCADE and GEMINI code calculations of the ^{4}He spectrum from the ^{3}He + Ag reaction at $E_{\rm Lab}(^3{\rm He}) = 90$ MeV and the corresponding fit (smooth line) using Eq. (1). The GEMINI calculations have been normalized to match with the CASCADE calculations.

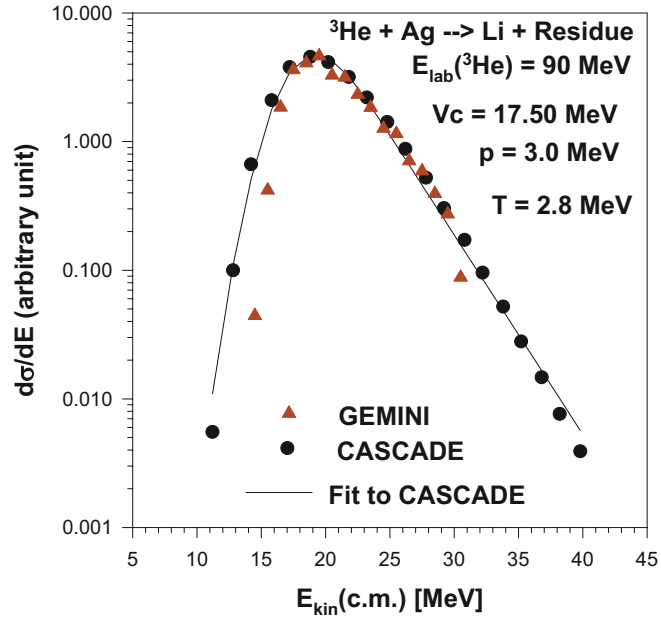

FIG. 7. (Color online) Statistical model CASCADE and GEMINI code calculations of the lithium spectrum from the ^{3}He + Ag reaction at $E_{\rm Lab}(^3{\rm He}) = 90$ MeV and the corresponding fit (smooth line) using Eq. (1). The GEMINI calculations have been normalized to match with the CASCADE calculations.

TABLE I. Comparison of temperature (T) and p parameters derived from the experimental and statistical model spectra.

System studied	Projectile energy (MeV) CN and E_X of CN (MeV)	Fragment investigated	Derived parameters			
			Experimental data		Statistical model calculation	
			p (MeV)	T (MeV)	p (MeV)	T (MeV)
$^{16}O + {}^{89}Y$	$E_{Lab}(^{16}O) = 96$ MeV	^{4}He	4.0 ± 0.4	2.90 ± 0.15	4.0	2.9
		Li	6.0 ± 0.6	4.50 ± 0.3	8.0	2.35
		Be	6.8 ± 1.0	3.6 ± 0.3	12.6	2.0
	^{105}Ag; $E_X = 76$ MeV	B	13.1 ± 1.0	3.35 ± 0.2	16.0	2.1
		C	15.0 ± 1.2	3.5 ± 0.3	20.0	2.2
$^{16}O + {}^{93}Nb$	$E_{Lab}(^{16}O) = 116$ MeV	^{4}He	3.5 ± 0.4	3.5 ± 0.1	4.0	3.4
		Li	3.9 ± 0.4	4.6 ± 0.2	11.0	2.8
		Be	10.9 ± 1.0	3.9 ± 0.2	19.0	2.4
	^{109}In; $E_X = 93.5$ MeV	B	11.8 ± 1.2	3.6 ± 0.2	25.0	2.3
		C	23.0 ± 1.0	3.5 ± 0.2	27.0	2.0
^{3}He + Ag	$E_{Lab}(^3He) = 90$ MeV	^{4}He	2.0 ± 0.2	3.0 ± 0.15	2.0	3.0
		Li	3.0 ± 0.3	5.8 ± 0.3	3.0	2.8
	$E_X \sim 82$ MeV with	B	8.0 ± 1.0	3.5 ± 0.2	7.0	2.6
	broad distribution	C	10.9 ± 1.0	3.5 ± 0.3	8.5	2.6

of the experiment are given in Ref. [9]. In the center-of-mass frame, the back-angle angular distributions of alpha, lithium, beryllium, boron, carbon etc. showed back-angle rises. The angular distributions of the heavier fragments such as carbon can be approximated by a $1/\sin\theta_{c.m.}$ function [9]. The angular distribution of lighter particles such as lithium can be fitted with an $a + b\cos^2\theta$ function as shown in Fig. 10. This kind of back-angle rise of the angular distributions for the lighter ions and approximate $1/\sin\theta_{c.m.}$ angular distribution for the heavier ions such as carbon are characteristics of statistical emission of the fragments [3,5] from an equilibrated compound nucleus. We have also studied the angle-integrated ratios of the yields of boron to carbon, beryllium to carbon and lithium to beryllium as a function of the exit-channel excitation energy for both $^{16}O + {}^{89}Y$ and $^{12}C + {}^{93}Nb$ reactions and find (Figs. 11 and 12) that the ratios of the yields of boron to carbon, beryllium to carbon and lithium to beryllium for $^{16}O + {}^{89}Y$ and $^{12}C + {}^{93}Nb$ reactions forming the same composite at the same excitation energy and similar spin distribution overlap with each other reasonably well, implying no significant

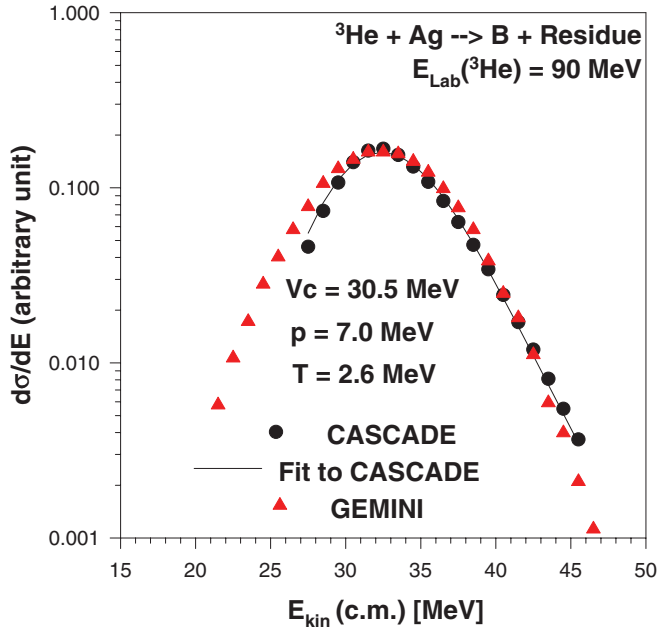

FIG. 8. (Color online) Statistical model CASCADE and GEMINI code calculations of the boron spectrum from the ^{3}He + Ag reaction at $E_{Lab}(^3He) = 90$ MeV and the corresponding fit (smooth line) using Eq. (1). The GEMINI calculations have been normalized to match with the CASCADE calculations.

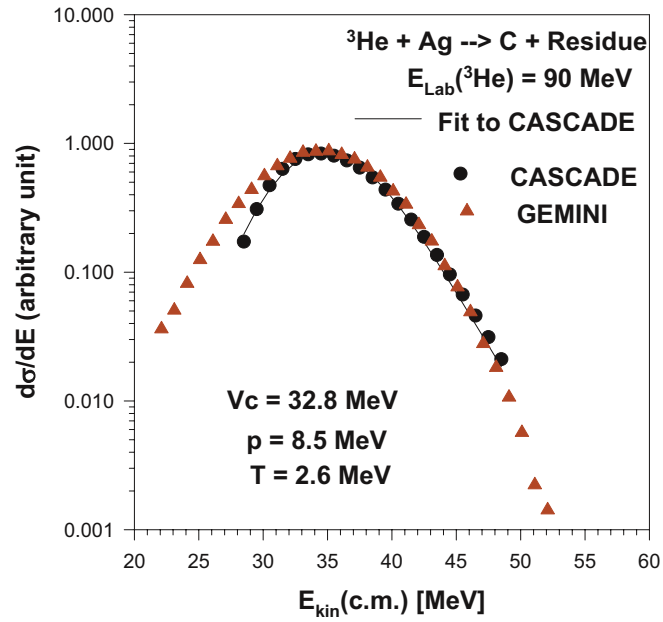

FIG. 9. (Color online) Statistical model CASCADE and GEMINI code calculations of the carbon spectrum from the ^{3}He + Ag reaction at $E_{Lab}(^3He) = 90$ MeV and the corresponding fit (smooth line) using Eq. (1). The GEMINI calculations have been normalized to match with the CASCADE calculations.

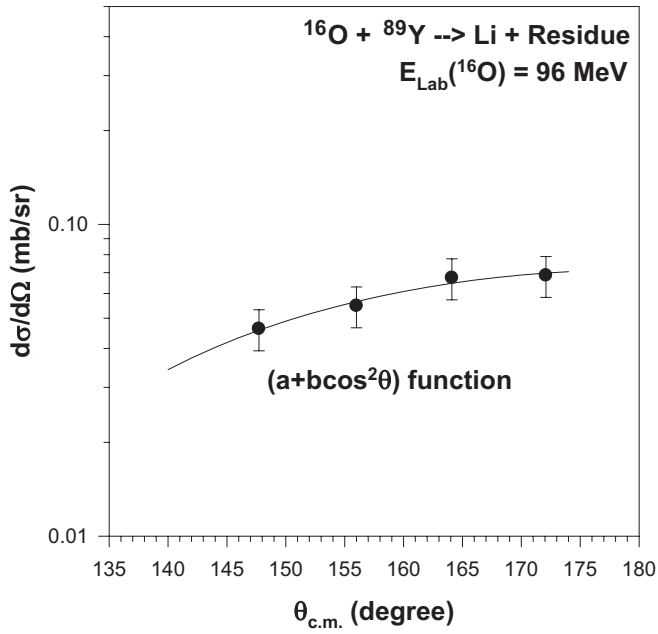

FIG. 10. Angular distribution of lithium particles integrated over the exit-channel excitation energy region ($0 \leqslant E_X < 43$ MeV) in the center-of-mass frame. The solid line is an $a + b\ \cos^2\theta$ function fit.

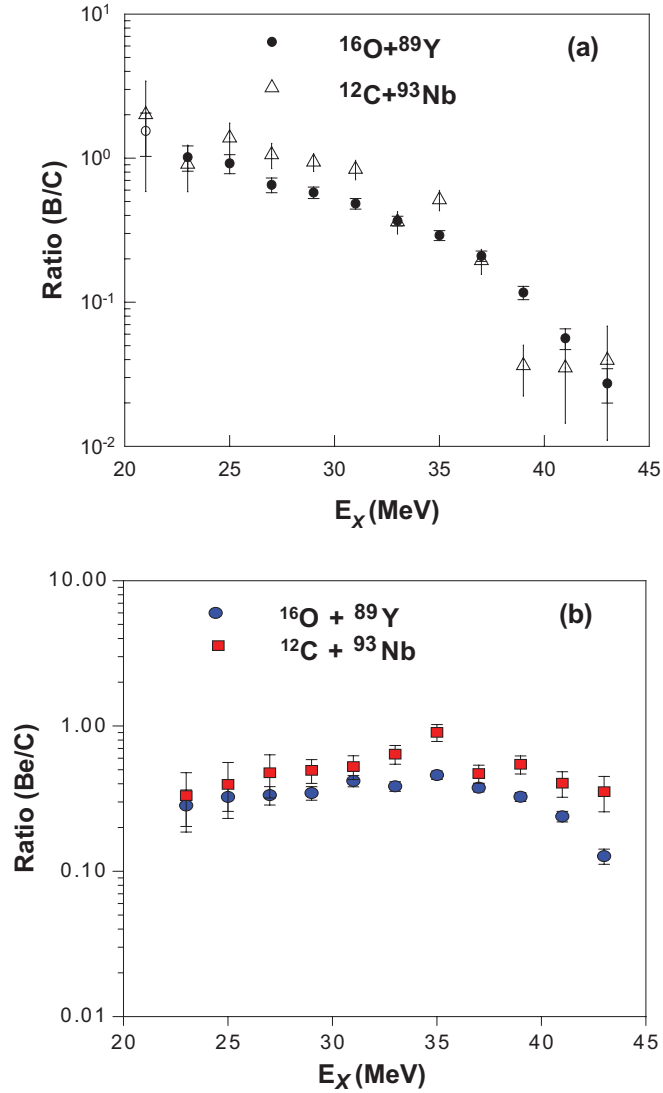

FIG. 11. (Color online) Angle-integrated ratios of (a) B/C and (b) Be/C versus exit-channel excitation energy for ^{16}O + ^{89}Y and ^{12}C + ^{93}Nb reactions producing ^{105}Ag at $E_X = 76$ MeV.

entrance-channel effect and hence their statistical origin from an equilibrated compound nucleus. The corresponding ratios did not overlap exactly due to the mismatch of the spin distributions of the compound nuclei formed by ^{16}O + ^{89}Y and ^{12}C + ^{93}Nb reactions. In Fig. 13, we show the overlayed lithium spectra at different angles from ^{12}C + ^{93}Nb and ^{16}O + ^{89}Y reactions after suitable normalizations. We find essentially identical spectral shape at different angles implying statistical emission of lithium particles at back angles. Similar results have also been obtained for other ions. The angular distributions show back-angle rise for all ions and tend to approximate $1/\sin\theta_{\text{c.m.}}$ function for heavier fragments such as carbon. So we have established that the emissions of the heavier fragments such as lithium, beryllium, boron and carbon from ^{16}O + ^{89}Y and ^{12}C + ^{93}Nb reactions at back angles (center-of-mass frame) are statistical.

In Fig. 14, we have overlayed the calculated (using the CASCADE code) and the experimental alpha spectra from the ^{16}O + ^{89}Y reaction at $E_{\text{Lab}}(^{16}\text{O}) = 96$ MeV and find that the shapes of the calculated and experimental alpha spectra are almost identical. A one-source fitting of the experimental alpha spectrum [using Eq. (1)] has been shown and the extracted temperature agrees very well with that obtained from the calculated statistical spectrum (Table I). The fitting of the alpha spectra with Eq. (1) was discussed earlier [8] and it was found that a one-source fit was reasonable, although a three-source fit with decreasing source temperature was definitely better. In Figs. 15–18, the experimental angle-integrated lithium, beryllium, boron, carbon spectra and the corresponding calculated statistical model spectra have been overlayed. The absolute normalizations of the experimental spectra have been obtained from the measured Rutherford elastic cross section at a suitable forward angle. The theoretical spectra have been normalized and shifted with respect to the corresponding experimental spectrum to overlay their peak positions. The experimental spectra have been fitted with Eq. (1) and T and p parameters have been extracted for each case. We find that the low-energy part of the heavy-ion spectra matches well, but the slopes of the calculated spectra are significantly steeper than the experimental spectra. The largest slope anomaly is seen for the lithium spectrum. In Table I, we show the fitted values of T and p obtained from statistical model calculations and the experimental spectra. We get very similar results from the study of alpha, lithium, beryllium, boron and carbon particles emitted at back angles from the ^{12}C + ^{93}Nb reaction at $E_{\text{Lab}}(^{12}\text{C}) = 85.5$ MeV forming the same compound nucleus ^{105}Ag at excitation energy = 76 MeV with very similar spin distribution. The first question is whether the presence of possible impurities in the target might cause the observed distortion of the slope of the back-angle spectra.

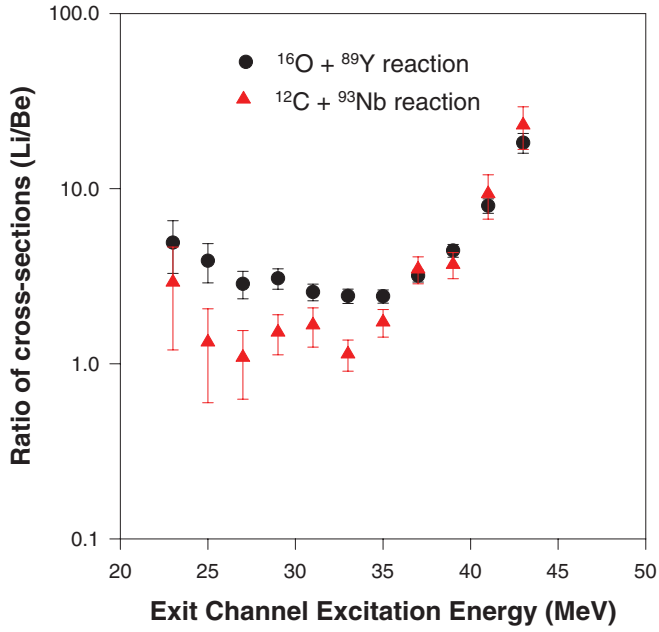

FIG. 12. (Color online) Angle-integrated ratios of Li/Be versus exit-channel excitation energy for ^{16}O + ^{89}Y and ^{12}C + ^{93}Nb reactions producing ^{105}Ag at $E_X = 76$ MeV.

The possible low-Z contaminants in the target are carbon and silicon that might come from the pump oil and oxygen. We did not see any observable presence of low-Z contaminants in the elastic yield measured by monitor detectors placed at forward angles. Moreover the kinetic energy of the emitted lithium and heavier fragments emitted at back angles from the reaction of oxygen with low-Z contaminants (carbon, oxygen, silicon) will be very low and they cannot possibly

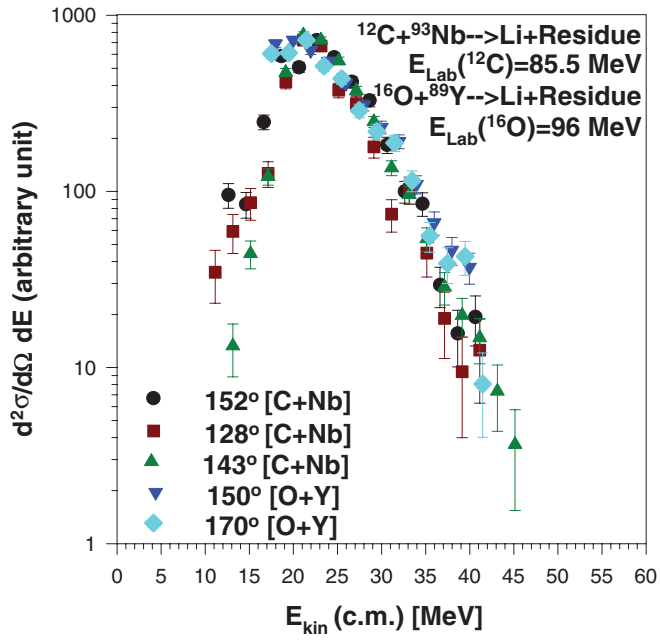

FIG. 13. (Color online) Overlay plots of lithium spectra (after suitable normalizations) at different angles for ^{12}C + ^{93}Nb and ^{16}O + ^{89}Y reactions forming ^{105}Ag at $E_X = 76$ MeV.

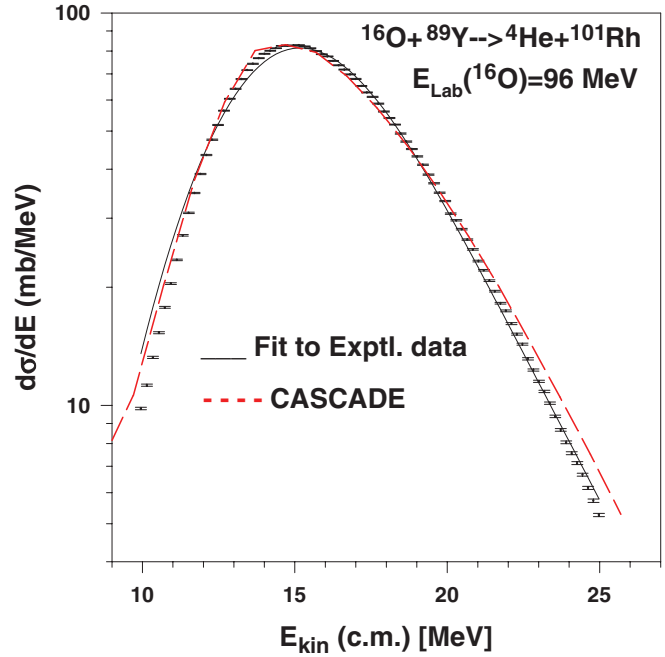

FIG. 14. (Color online) Overlay plots of experimental and theoretical statistical model spectra for alpha particles from the ^{16}O + ^{89}Y reaction at $E_{\rm Lab}(^{16}{\rm O}) = 96$ MeV and the corresponding fit to the experimental spectrum using Eq. (1). The theoretical spectrum has been normalized and shifted with respect to the corresponding experimental spectrum to overlay their peak positions. The solid black curve represents the fit to the experimental data points. The dashed red curve shows statistical model CASCADE code calculations.

produce any significant effect in the high-energy tail of the fragments emitted at back angles from ^{16}O + ^{89}Y and ^{12}C + ^{93}Nb reactions. They might slightly contaminate the low-energy part of the observed spectra, but no significant anomalies have been observed in the lower energy side of the heavy fragment spectra. So the effect of any such low-Z contaminant can be neglected. High-Z contaminants such as tantalum and dysprosium might be present in the target at a level of $<$100 ppm (as per foil supplier's catalogue). However, the cross sections of lithium and heavier fragments emitted at back angles from the reaction of oxygen with such high-Z contaminants should be orders of magnitude lower than the corresponding cross sections from the ^{16}O + ^{89}Y reaction, because of the Coulomb barrier effect. Moreover such high-Z contaminants should produce colder spectra. So the observed anomaly of the high-energy tail of the emitted heavy fragments from ^{16}O + ^{89}Y and ^{12}C + ^{93}Nb reactions cannot be due to the presence of the small amount of contaminants in the target.

It might be argued that the observed mismatch of the slopes of the calculated and experimental spectra indicates nonstatistical emission of the fragments in the high-energy tail region. However, the angular distributions of the tail region of the spectra are not different from the angular distribution of the total spectra, and Fig. 13 shows that the spectral shapes of lithium particles are almost identical at different angles. We do not see any significant entrance-channel dependence in the high-energy tail region of the heavy-ion spectra from

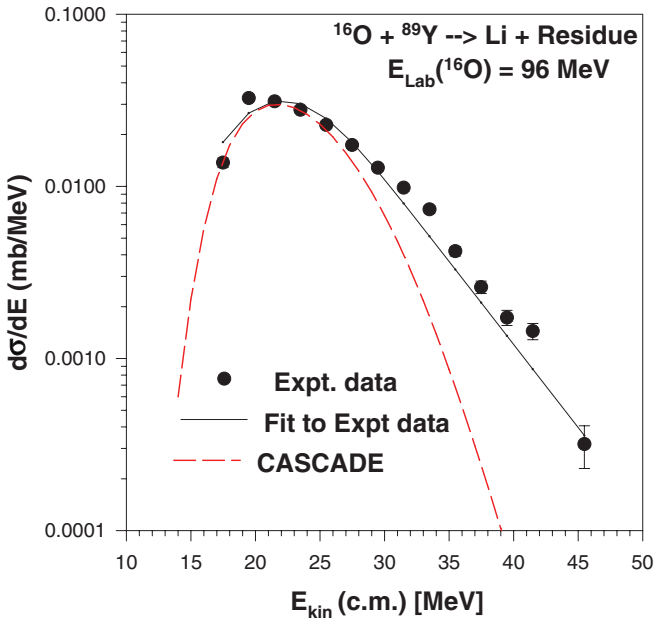

FIG. 15. (Color online) Overlay plots of experimental and theoretical statistical model spectra for lithium particles from the ^{16}O + ^{89}Y reaction at E_{Lab}(^{16}O) = 96 MeV and the corresponding fit to the experimental spectrum using Eq. (1). The theoretical spectrum has been normalized and shifted with respect to the corresponding experimental spectrum to overlay their peak positions. The solid black curve represents the fit to the experimental data points. The dashed red curve shows statistical model CASCADE code calculations.

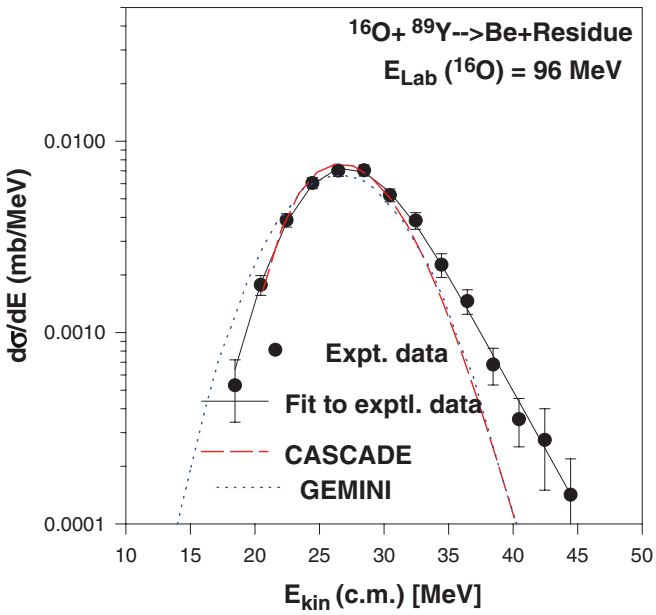

FIG. 16. (Color online) Overlay plots of experimental and theoretical statistical model spectra for beryllium particles from the ^{16}O + ^{89}Y reaction at E_{Lab}(^{16}O) = 96 MeV and the corresponding fit to the experimental spectrum using Eq. (1). The theoretical spectrum has been normalized and shifted with respect to the corresponding experimental spectrum to overlay their peak positions. The solid black curve represents the fit to the experimental data points. The dashed red curve and dotted blue curve show statistical model CASCADE code and GEMINI code calculations respectively.

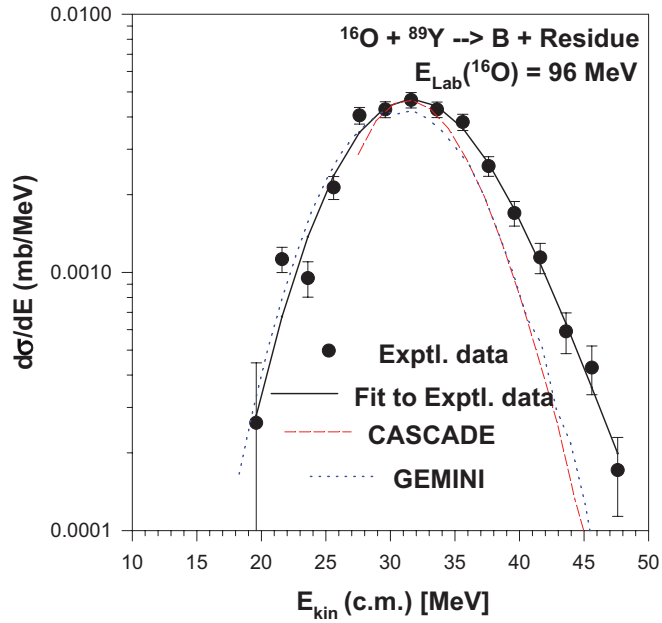

FIG. 17. (Color online) Overlay plots of experimental and theoretical statistical model spectra for boron particles from the ^{16}O + ^{89}Y reaction at E_{Lab}(^{16}O) = 96 MeV and the corresponding fit to the experimental spectrum using Eq. (1). The theoretical spectrum has been normalized and shifted with respect to the corresponding experimental spectrum to overlay their peak positions. The solid black curve represents the fit to the experimental data points. The dashed red curve and dotted blue curve show statistical model CASCADE code and GEMINI code calculations respectively.

Figs. 11 and 12. So there is no indication of any significant nonstatistical emission process in the high-energy tail region.

There is a question whether orbiting reactions [10,11] might be responsible for the observed slope anomaly, because the angular distributions of the emitted fragments show back-angle rise in the case of orbiting reactions also. However, in the case of orbiting processes, a strong entrance-channel effect was seen [9,10] and that is absent in this case (Figs. 11 and 12). Moreover, in the case of orbiting reactions, although all the degrees of freedom (such as the shape of the orbiting composite) are not equilibrated, temperature equilibration is attained. So the spectral shape of the orbiting fragments is expected to be similar [11] to that from the statistical model calculations, although the absolute yield of the orbiting fragments is much higher than the estimates from the statistical model calculations. There is no known reaction mechanism that can produce back-angle rise of the angular distributions of the emitted fragments, but the nuclei fail to attain at least thermal equilibration. The thermal equilibration implies that the spectral shape of the emitted fragments would be similar to that expected from the statistical model calculations. So the observed slope anomaly (Figs. 15–18) cannot be explained by orbiting or similar reaction mechanisms.

In order to further check whether the observed slope anomaly of the back-angle heavy-ion spectra from ^{16}O + ^{89}Y and ^{12}C + ^{93}Nb reactions are characteristics of those particular reactions or a more general feature of the statistical heavy ion emission process, we have compared back-angle

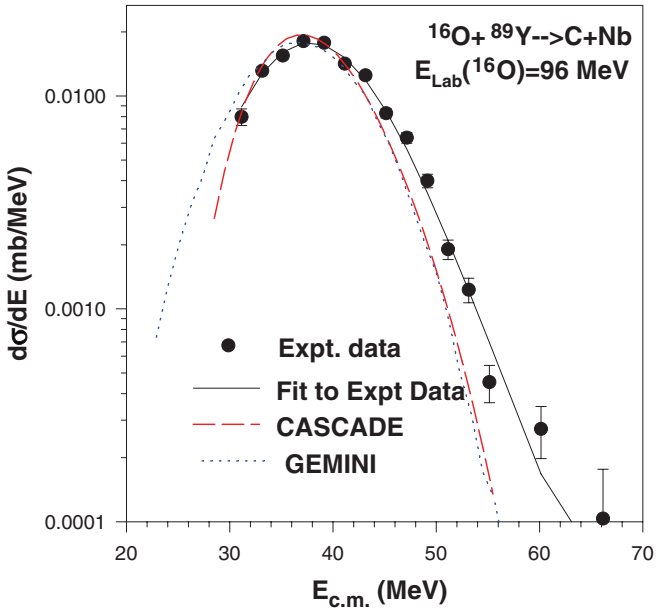

FIG. 18. (Color online) Overlay plots of experimental and theoretical statistical model spectra for carbon particles from the $^{16}O + {}^{89}Y$ reaction at $E_{Lab}(^{16}O) = 96$ MeV and the corresponding fit to the experimental spectrum using Eq. (1). The theoretical spectrum has been normalized and shifted with respect to the corresponding experimental spectrum to overlay their peak positions. The solid black curve represents the fit to the experimental data points. The dashed red curve and dotted blue curve show statistical model CASCADE code and GEMINI code calculations respectively.

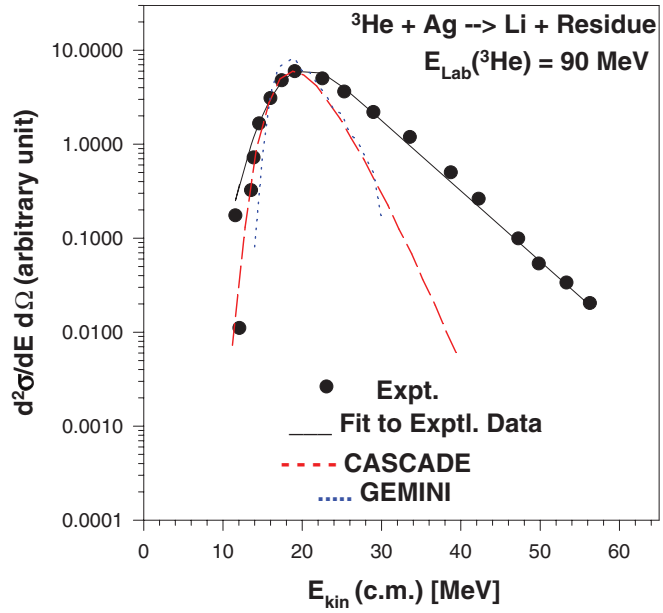

FIG. 19. (Color online) Overlay plots of experimental and theoretical statistical model spectra for lithium particles from the $^{3}He + Ag$ reaction at $E_{Lab}(^{3}He) = 90$ MeV and the corresponding fit to the experimental spectrum using Eq. (1). The theoretical spectrum has been normalized and shifted with respect to the corresponding experimental spectrum to overlay their peak positions. The solid black curve represents the fit to the experimental data points. The dashed red curve and dotted blue curve show statistical model CASCADE code and GEMINI code calculations respectively.

heavy-ion evaporation spectra from the $^{3}He + Ag$ reaction at $E_{Lab}(^{3}He) = 90$ MeV [3] with the CASCADE and GEMINI code calculations. The temperature ($T = 3.0$ MeV) and p value ($p = 2.0$ MeV) obtained from the calculated ^{4}He spectrum [Fig. 6] agree very well with the corresponding parameters obtained from the experimental ^{4}He spectrum of the $^{3}He + Ag$ reaction at $E_{Lab}(^{3}He) = 90$ MeV taken at back angle [7]. The angular distribution [3] of the emitted heavy ions (lithium, beryllium, boron, and carbon) from the $^{3}He + Ag$ reaction at $E_{Lab}(^{3}He) = 90$ MeV showed back-angle rises, and they tended toward an approximate $1/\sin\theta_{c.m.}$ function for the heavier fragments. As discussed in Ref. [3], these kinds of angular distributions at back angles indicate the statistical origin of those fragments. In Figs. 19–21, we show overlayed plots of calculated lithium, boron, and carbon evaporation spectra along with the corresponding experimental spectra taken at back angle from Ref. [3]. The experimental spectra have been fitted with Eq. (1) and the values of T and p parameter have been extracted for each case. As before, we find that the slopes of the calculated heavy fragments are significantly steeper than the corresponding slopes obtained from the experimental spectra, and the slope anomaly is the largest for the lithium spectrum. The results have been tabulated in Table I. Preequilibrium emission of neutrons is expected from this reaction, and it produces a broad distribution of the excitation energy of the compound nucleus around a mean value of ~82 MeV [3]. The statistical model calculations do not consider any preequilibrium neutron emission and so the temperature extracted from the calculated statistical model spectra should give an upper limit of the temperature. The consideration of a distribution of excitation energy around 82 MeV should increase the slope anomaly. At higher excitation energy (150–200 MeV), reasonable agreements [4] with the statistical model calculations have been obtained. The shapes of the heavy ion spectra (beryllium, boron, carbon) emitted at back angles from the $^{3}He + Ag$ reaction at $E_{Lab}(^{3}He) = 198.6$ MeV agree reasonably well [4] with the corresponding spectra calculated from the statistical model codes. The temperatures were obtained by fitting the spectra with Eq. (1), and temperatures around $T \approx 4$ MeV were obtained from both the alpha and heavy-ion spectra. In Fig. 22, we show the overlayed calculated (GEMINI) and experimental boron spectra for the $^{3}He + Ag$ reaction at $E_{Lab}(^{3}He) = 198.6$ MeV [4]. The calculated and experimental spectra match reasonably well, showing that the slope anomaly disappears at high excitation energy.

We also performed an experimental study of the back-angle heavy-ion emission from the $^{16}O + {}^{93}Nb$ reaction at $E_{Lab}(^{16}O) = 116$ MeV. A 5 p nA ^{16}O beam from the Variable Energy Cyclotron Center, Kolkata, at $E_{Lab}(^{16}O) = 116$ MeV was used to bombard a 1 mg/cm^2 thick ^{93}Nb foil and alpha, lithium, beryllium, boron, and carbon spectra were recorded. The details of the experiment are given in Ref. [9]. In Figs. 23 and 24, we show overlayed plots of calculated and experimental alpha and lithium spectra. The spectral shapes of the alpha spectra match reasonably well. However, as before,

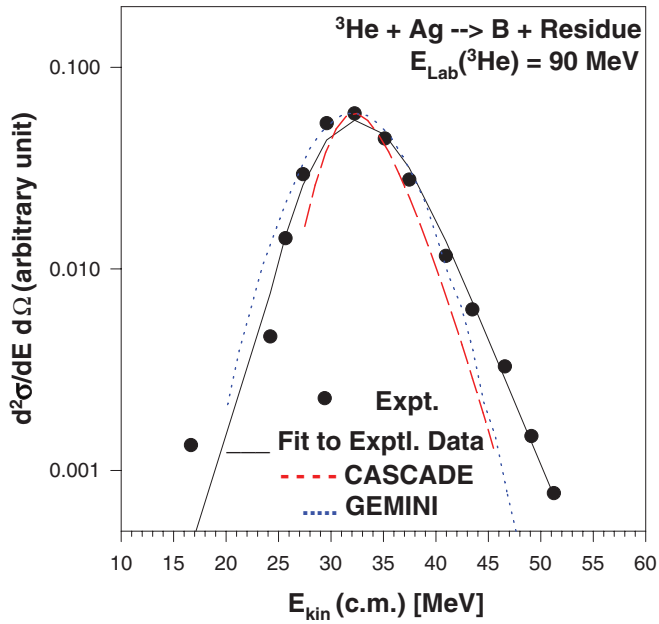

FIG. 20. (Color online) Overlay plots of experimental and theoretical statistical model spectra for boron particles from the ^{3}He + Ag reaction at $E_{Lab}(^3He) = 90$ MeV and the corresponding fit to the experimental spectrum using Eq. (1). The theoretical spectrum has been normalized and shifted with respect to the corresponding experimental spectrum to overlay their peak positions. The solid black curve represents the fit to the experimental data points. The dashed red curve and dotted blue curve show statistical model CASCADE code and GEMINI code calculations respectively.

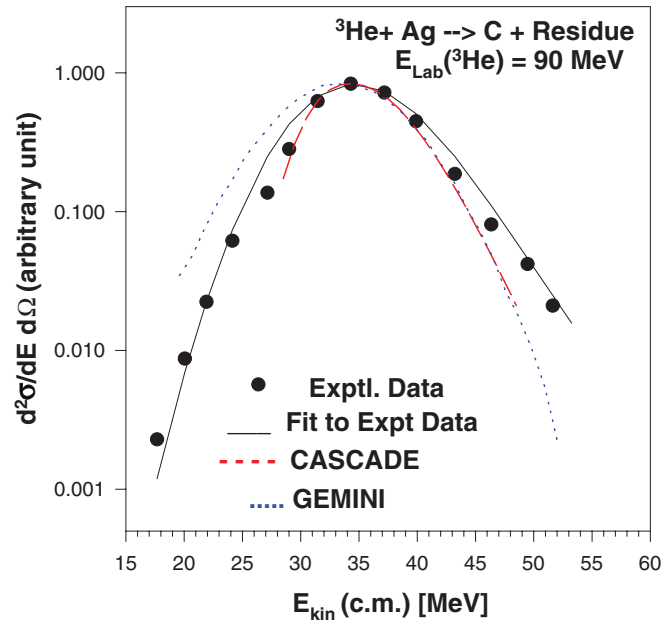

FIG. 21. (Color online) Overlay plots of experimental and theoretical statistical model spectra for carbon particles from the ^{3}He + Ag reaction at $E_{Lab}(^3He) = 90$ MeV and the corresponding fit to the experimental spectrum using Eq. (1). The theoretical spectrum has been normalized and shifted with respect to the corresponding experimental spectrum to overlay their peak positions. The solid black curve represents the fit to the experimental data points. The dashed red curve and dotted blue curve show statistical model CASCADE code and GEMINI code calculations respectively.

the slope of the calculated lithium spectrum is significantly steeper compared to that of the experimental spectrum. In Figs. 25–27, we show the overlayed plots of the calculated and experimental (angle-integrated) beryllium, boron and carbon spectra. We find from Fig. 24–27 that the slope of the calculated spectrum is always steeper than the corresponding experimental spectrum and the deviation is in the tail region, although there is reasonable agreement between the calculated and experimental spectra in the rest of the spectrum. The extracted slope parameter (T) of the calculated spectrum has always been found to be lower than the corresponding T parameter extracted from the experimental spectrum as shown in Table I. In the case of the overlayed experimental and statistical model spectra (Figs. 14–27), the calculated spectra were typically shifted by 0.5–1.5 MeV to match with the peak positions of the corresponding experimental spectra. Larger shifts (∼4 MeV) of the calculated beryllium and boron spectra towards the lower energy were required for ^{16}O + ^{89}Y and ^{16}O + ^{93}Nb reactions implying deformation of the residual nuclei. No normalization factor was required for calculated alpha and carbon spectra; however, large normalization factors (factor of 10 or more) were required for calculated beryllium and boron spectra, because the optical model potentials required to calculate the transmission coefficients of beryllium and boron are poorly known. The absolute cross section of the emitted fragments depends very strongly on the transmission coefficients and it is possible to change the absolute cross sections of the weak channels by orders of magnitude by

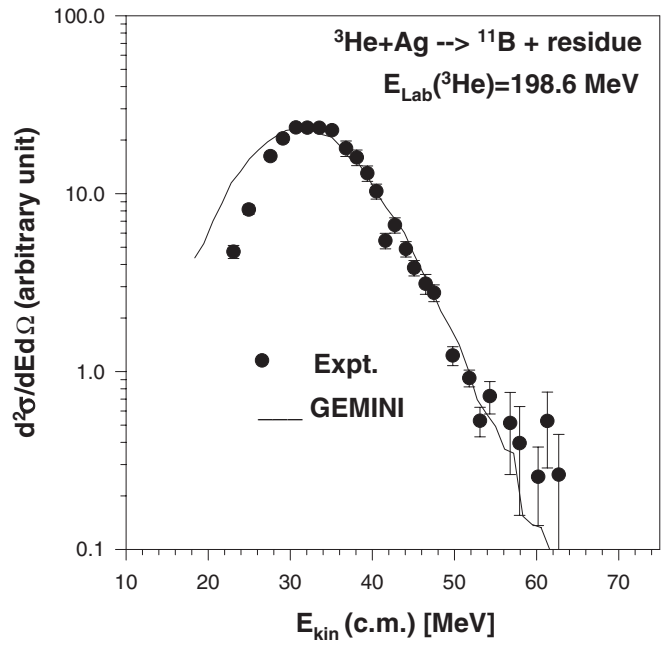

FIG. 22. Overlay plots of experimental and theoretical statistical model spectra for boron particles from the ^{3}He + Ag reaction at $E_{Lab}(^3He) = 198.6$ MeV. The theoretical (GEMINI) spectrum has been normalized and shifted with respect to the corresponding experimental spectrum to overlay their peak positions.

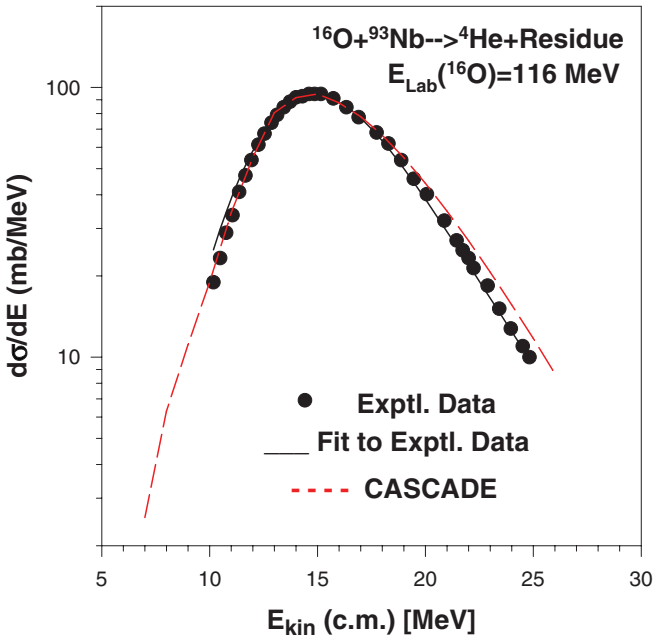

FIG. 23. (Color online) Overlay plots of experimental and theoretical statistical model spectra for alpha particles from the $^{16}O + {}^{93}Nb$ reaction at $E_{Lab}(^{16}O) = 116$ MeV and the corresponding fit to the experimental spectrum using Eq. (1). The theoretical spectrum has been normalized and shifted with respect to the corresponding experimental spectrum to overlay their peak positions. The solid black curve represents the fit to the experimental data points. The dashed red curve shows statistical model CASCADE code calculations.

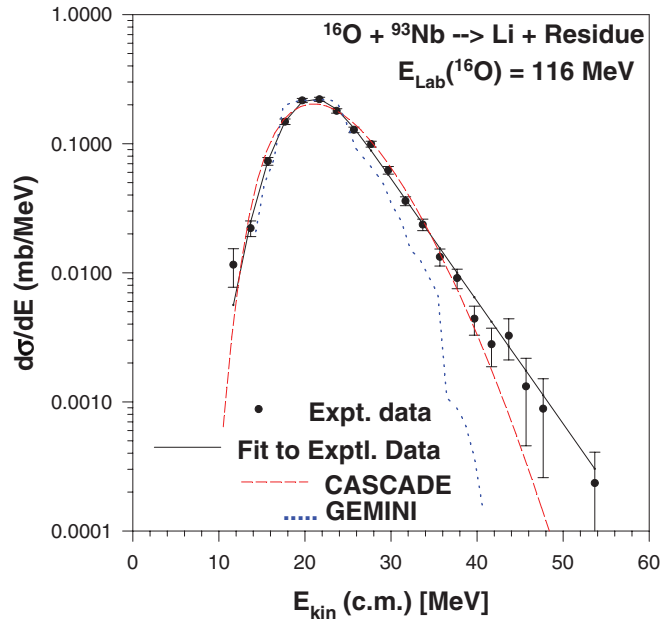

FIG. 24. (Color online) Overlay plots of experimental and theoretical statistical model spectra for lithium particles from the $^{16}O + {}^{93}Nb$ reaction at $E_{Lab}(^{16}O) = 116$ MeV and the corresponding fit to the experimental spectrum using Eq. (1). The theoretical spectra (CASCADE and GEMINI) have been normalized and shifted with respect to the corresponding experimental spectrum to overlay their peak positions. The solid black curve represents the fit to the experimental data points. The dashed red curve and dotted blue curve show statistical model CASCADE code and GEMINI code calculations respectively.

choosing different optical model potentials for calculating the transmission coefficients. However, the spectral shapes (particularly the T parameter) remain about the same for different sets of the transmission coefficients. So we have emphasized the comparison of the corresponding spectral shapes. The experimental spectra were fitted with Eq. (1), and T and p parameters were extracted for each case. As before, we find that the slopes of the calculated spectra are steeper than those obtained from the experimental spectra, but the slope anomaly has decreased somewhat compared to lower energy data taken at $E_{Lab}(^{16}O) = 96$ MeV. In Table I, we have presented the fitted values of T and p for both the statistical model and the experimental spectra. In Figs. 23–27, both the CASCADE and GEMINI calculations producing similar spectral shapes are shown.

We find from our study of the back-angle alpha and heavy-ion spectra from the $^{16}O + {}^{89}Y$ reaction at $E_{Lab}(^{16}O) =$ 96 MeV, the $^{12}C + {}^{93}Nb$ reaction at $E_{Lab}(^{12}C) = 85.5$ MeV, the $^{16}O + {}^{93}Nb$ reaction at $E_{Lab}(^{16}O) = 116$ MeV and the $^{3}He + Ag$ reaction at $E_{Lab}(^{3}He) = 90$ and 198.6 MeV that the experimental and calculated alpha spectra (from the statistical models) agree well in all the cases. However, the experimental heavy ion spectra show significantly gentler slope than the calculated statistical spectra. This anomaly is largest for the lithium spectra and decreases as the excitation energy of the compound nucleus increases. The qualitative features of this anomaly are the same for ^{16}O, ^{12}C and ^{3}He induced reactions. The observed back-angle rise of the angular distribution and the lack of any entrance channel dependence of the reaction products imply the statistical origin of these reaction products. If reaction dynamics is responsible for the slope anomaly, the anomalies should be qualitatively different for ^{16}O and ^{3}He induced reactions. The observation of a very similar slope anomaly for both the ^{16}O and ^{3}He induced reactions indicates that the reaction dynamics should not be responsible for the anomalies.

IV. DISCUSSION

The shapes of the calculated statistical model spectra are very robust and do not depend on deformation parameters, transmission coefficients, critical angular momentum etc. The level-density parameter of the statistical model is essentially the only parameter that can change the slope of the fragment spectra. It is known [1] that there is no excitation-energy dependence of the level-density parameter in the $A \approx$ 100 mass region. Even if we introduce any excitation-energy dependence of the level-density parameter, it cannot explain the observed features: no anomaly for the alpha spectrum, very significant slope anomaly for the lithium spectrum, and somewhat smaller anomalies for other heavier particle spectra. An additional angular momentum dependence of the nuclear level density can be introduced by multiplying the liquid-drop moment of inertia by a factor. If we multiply

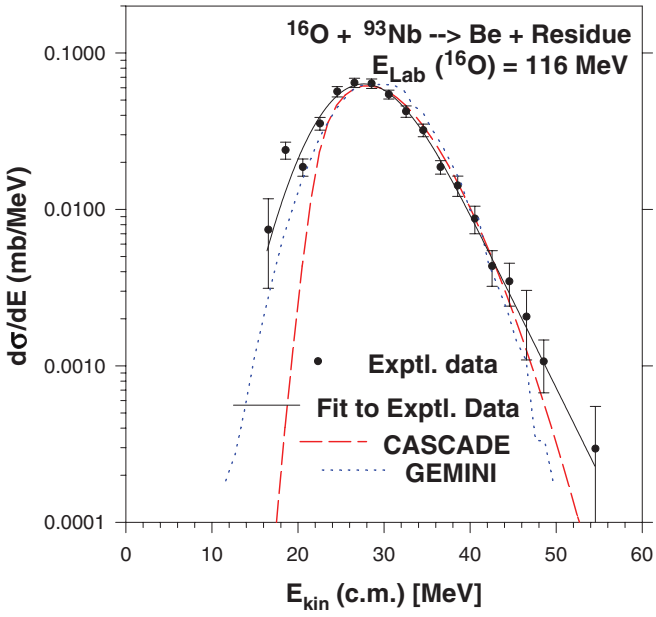

FIG. 25. (Color online) Overlay plots of experimental and theoretical statistical model spectra for beryllium particles from the ^{16}O + ^{93}Nb reaction at $E_{\rm Lab}(^{16}{\rm O}) = 116$ MeV and the corresponding fit to the experimental spectrum using Eq. (1). The theoretical spectra (CASCADE and GEMINI) have been normalized and shifted with respect to the corresponding experimental spectrum to overlay their peak positions. The solid black curve represents the fit to the experimental data points. The dashed red curve and dotted blue curve show statistical model CASCADE code and GEMINI code calculations respectively.

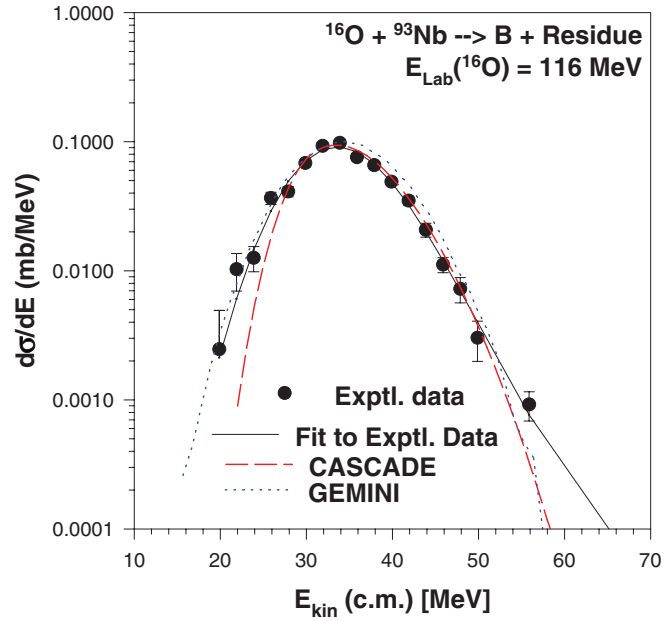

FIG. 26. (Color online) Overlay plots of experimental and theoretical statistical model spectra for boron particles from the ^{16}O + ^{93}Nb reaction at $E_{\rm Lab}(^{16}{\rm O}) = 116$ MeV and the corresponding fit to the experimental spectrum using Eq. (1). The theoretical spectra (CASCADE and GEMINI) have been normalized and shifted with respect to the corresponding experimental spectrum to overlay their peak positions. The solid black curve represents the fit to the experimental data points. The dashed red curve and dotted blue curve show statistical model CASCADE code and GEMINI code calculations respectively.

the liquid-drop moment of inertia by 0.9, then the cross section of ^{12}C increases by an order of magnitude for $^{16}{\rm O} + ^{89}{\rm Y}$ reaction at $E_{\rm Lab}(^{16}{\rm O}) = 96$ MeV, but the slope of the ^{12}C spectrum becomes only a little bit gentler, increasing the extracted temperature from 1.7 to 2.2 MeV. The corresponding effects on the cross sections and the extracted temperatures from the boron, beryllium, lithium and alpha spectra become progressively smaller as those particles carry progressively lower orbital angular momentum. So such angular momentum dependence of the nuclear level density cannot explain why the slope anomaly is largest for the lithium that carries much lower orbital angular momentum than ^{12}C, whereas there is no anomaly for the alpha spectrum. So we think that the observed slope anomalies found from both the literature data [3] and our data cannot be explained by adjusting the parameters of the statistical model or by reaction dynamics.

There is also a question whether the slope anomaly might be due to the production of the observed fragments from the sequential decay of the prefragments. According to the GEMINI code, such an effect should be largest for the lithium spectra. The GEMINI code calculations have been done considering such effect and no significant change of the slope parameter (T) has been found compared to the corresponding (CASCADE code) evaporation spectrum (Figs. 2, 7, 19, and 24). Moreover, such sequential decay of the prefragments should increase at higher excitation energy. So if the observed slope anomaly is due to the sequential decay of the prefragments, then the disagreement between the experimental slope parameter (T) and that obtained from the calculated evaporation spectrum (CASCADE code) should increase at higher excitation energy contrary to the observations.

A. Effect of shape polarization

Let us examine if Moretto's shape polarization model [5] for the emission of large fragments from a compound nucleus might explain the observed anomalies. On the basis of this model, Moretto deduced [5] Eq. (1) describing the shape of kinetic-energy spectrum of the emitted heavy-ion spectra from a compound nucleus. The equation contains three parameters, p, T, and V_C, and they are interrelated by the relation $\Delta V_C = 2\sqrt{pT}$, where ΔV_C denotes the fluctuations of the Coulomb barrier. However, the model does not give any *ab initio* method to calculate p and T parameters. We fitted our experimental and statistical model spectra with Eq. (1) and extracted T, p and V_C parameters. There is interplay between T and p parameters and the decrease of the p parameter can increase the T parameter. We performed best fits by minimizing corresponding chi-square values and checked that if we decrease p by a significant amount and try to fit the spectra by increasing T, then no reasonable fit can be obtained for lithium, beryllium, boron, and carbon spectra.

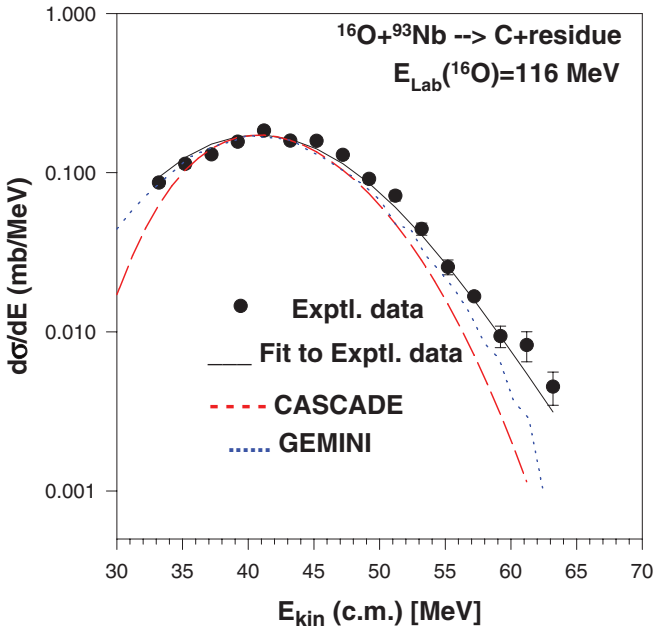

FIG. 27. (Color online) Overlay plots of experimental and theoretical statistical model spectra for carbon particles from the $^{16}O + {}^{93}Nb$ reaction at $E_{Lab}(^{16}O) = 116$ MeV and the corresponding fit to the experimental spectrum using Eq. (1). The theoretical spectra (CASCADE and GEMINI) have been normalized and shifted with respect to the corresponding experimental spectrum to overlay their peak positions. The solid black curve represents the fit to the experimental data points. The dashed red curve and dotted blue curve show statistical model CASCADE code and GEMINI code calculations respectively.

In order to study the effect of shape polarization, let us first assume that both the residual and ejectile nuclei are spherical and the distance between the centers of the two nuclei is r when they are in a touching configuration. So we obtain $V_C = \frac{Z_{res}Z_{ejec}}{r}$, where Z_{res} and Z_{ejec} denote the atomic numbers of the residual and ejectile nuclei respectively. Then (assuming no change of the spherical shape), we obtain $\Delta V_C = -\frac{Z_{res}Z_{ejec}}{r^2}\Delta r$. Following Refs. [5,7], we assume $\Delta r \propto \sqrt{T}$ (considering r as the deformation parameter) and then obtain using the equation $\Delta V_C = 2\sqrt{pT}$ the following relationship:

$$p \propto \frac{(Z_{res}Z_{ejec})^2}{r^4}. \quad (2)$$

From Eq. (2), we obtain the result that the ratio of the p parameters for carbon (p_C) and helium (p_{He}) spectra should be 5.25 for the $^{16}O + {}^{89}Y$ reaction, whereas the corresponding ratios extracted by fitting the experimental and statistical model spectra are $= 3.75 \pm 0.5$ and 4.5 respectively. In the case of emission of the lithium particles from the $^{16}O + {}^{89}Y$ reaction, we obtain from Eq. (2) $(p_{Li}/p_{He}) = 1.9$, whereas the corresponding ratios obtained from both the experimental and statistical model spectra are 1.5 ± 0.2 and 1.5 respectively. In the case of the $^3He + Ag$ reaction, the calculated ratio of $p_C/p_{He} = 4.88$ using Eq. (2), whereas the corresponding ratios obtained by fitting the experimental and statistical model spectra are $= 5.45 \pm 0.75$ and 4.25 respectively. We think that the increase of the p value (for heavier ejectiles) as obtained by fitting the experimental spectra with Eq. (1) is in qualitative agreement with our simple estimates from Eq. (2). Somewhat lower values of the ratios obtained from the experimental spectra of the $^{16}O + {}^{89}Y$ reaction compared to the estimates from Eq. (2) might be due to the shape polarization effect that should reduce the value of the p parameter compared to the estimates of Eq. (2), that is based on the assumption of spherical nuclei with no shape polarization. So shape polarization should reduce the value of the p parameter (from the assumption of spherical shape) for large fragments and there might be some qualitative evidence for such an effect from the experimental spectra of heavier fragments from the $^{16}O + {}^{89}Y$ reaction. Let us now examine the possible effect of the shape polarization on the spectral temperature (T). According to the shape polarization model of Moretto [5], the temperature (T) is proportional to the square of the fluctuation of the deformation coordinate, i.e. $T \propto (\Delta r)^2$. The fluctuation of the deformation coordinate will certainly be larger for the emission of the larger fragments. So the shape polarization effect should tend to increase the spectral temperature obtained from the spectra of the larger fragments. Hence, according to this argument, the shape polarization effect should be more important for the carbon emission than the lithium emission. However, experimentally, we have found that the slope anomaly is largest for the lithium spectrum and the highest spectral temperature has been extracted from the lithium spectrum. The effect of shape polarization should not be less important at higher excitation energy. However, it has been observed that the slope anomaly decreases rapidly at higher excitation energy and it is not visible around $E_X \sim$ (150–200) MeV. So we think that the inclusion of the shape polarization effect in a statistical model might not explain the observed results. However, at present there is no statistical model that includes the effect of shape polarization. Such models should be developed and compared with our experimental results.

B. Classical fission delay due to nuclear viscosity

Another point to examine is whether the time delay of the emission of large fragments from the compound nucleus (similar to fission delay) because of the effect of the viscosity of the nuclear medium might affect the spectral temperature of the fragment. The observation of relatively long fission time ($\sim 10^{-20}$ s) of the excited high-Z compound nuclei from neutron multiplicity measurements led to the speculation that the viscosity of the hot nuclear medium might be responsible [12–14] for slowing down evolution from the equilibrated compound nuclear shape to the scission point. At higher excitation energy, the hypothesis requires much higher values of the viscosity parameter to explain neutron prescission multiplicity data. Recently McCalla and Lestone [15] proposed a different model without increasing the viscosity parameter steeply with the temperature for relatively lower Z nuclei (Po) where the fission barrier is not very low. However, direct measurements by x-ray and crystal blocking techniques have shown very long fission delay times ($\sim 10^{-18}$ s) even for the highly excited

uranium-like and transuranium nuclei [16–18]. These results have not so far been explained by the viscosity effect.

If we consider that the emissions of the fragments such as lithium, beryllium, carbon etc. from the $^{16}O + {}^{89}Y$ and $^{3}He + Ag$ reactions are delayed by the viscosity effect slowing down the evolution of the equilibrated compound nucleus to scission point, then the spectral temperatures of the fragments should be lower than the expectations from the standard statistical model predictions, because of the emission of prescission neutrons during the long evolution time period. So the consideration of any such classical time delay effect should certainly produce a colder spectrum compared to the standard statistical model predictions, contrary to our observations. So the observed higher spectral temperatures of the fragments compared to the statistical model predictions cannot be explained by classical time delay effects (such as due to the nuclear viscosity), because such effects should produce lower temperature, because of the emission of the prescission neutrons.

V. CONCLUSION

We have studied experimentally the statistical emission of alpha and heavier fragments produced in low-energy (4–8 MeV/A) ^{16}O and ^{12}C induced nuclear reactions at back angles. We have compared our experimental fragment spectra and the existing back-angle experimental statistical fragment spectra from the $^{3}He + Ag$ reactions at $E_{Lab}(^{3}He) = 90$ MeV and $E_{Lab}(^{3}He) = 198.6$ MeV [3,4] with the statistical model calculations. The observed shapes of the alpha-particle spectra agree with the corresponding statistical model calculation in all the cases. However, the temperatures extracted from the slopes of the spectra of the heavier fragments are significantly higher than the expectations from the statistical model. The anomaly is largest for the lithium spectrum and all the slope anomalies decrease at higher excitation energy for all the reactions studied. The observed similarity of the slope anomalies for two very different entrance channels (^{16}O and ^{3}He induced reactions) indicates that the reaction dynamics is unlikely to be the reason behind the observed slope anomalies. The anomalies cannot be understood by adjusting the parameters of the statistical model or using any other reaction model.

As a suggestion for future studies, we think the statistical model should be examined from a quantum mechanical perspective. A compound nuclear wave function is a superposition of all possible exit-channel dinuclear state wave functions, where each dinuclear state wave function (a quasibound state of a heavy-ion fragment and residual nucleus) undergoes exponential decay in time with a Breit-Wigner width. A dinuclear state comprising lithium and the corresponding residual nucleus should have a large Breit-Wigner width because of the large break-up probability of lithium in the nuclear and Coulomb field of the residual nucleus, whereas a dinuclear state comprising an alpha particle and the residual nucleus should be relatively stable with a small Breit-Wigner width. A large Breit-Wigner width can affect the entropy function and, hence, the related temperature of the exit-channel configuration. If the temperature is calculated by convoluting the entropy function with a Breit-Wigner function of large width, then a higher temperature is obtained. A quantum state even with a large Breit-Wigner width could have nonexponential, almost flat initial survival probability for some time [19–22], allowing fragments such as lithium to achieve statistical equilibration and come out of the nuclear vicinity without decaying. Although nonexponential decay characteristics have not yet been observed [23] in nuclear physics in direct experiments because of their expected very short time scale [of the order of $\geqslant \hbar/$(energy release)], the nonexponential nuclear decay time scales might be comparable to the lifetime of highly excited compound nuclei and play a role in their decays.

ACKNOWLEDGMENTS

We thank R. Vandenbosch (University of Washington), J. N. De (Saha Institute of Nuclear Physics, Kolkata, India) and S. K. Samaddar (Saha Institute of Nuclear Physics, Kolkata, India) for a critical reading and useful discussion of our manuscript. We thank D. R. Chakrabarty (Nuclear Physics Division, Bhabha Atomic Research Center, Mumbai, India) for performing CASCADE code calculations and useful discussions. A. De acknowledges the support received from the UGC [Ref. No. F.PSW-011/07-08(ERO)] and collaborative research Scheme No. UGC-DAE-CSR-KC/CRS/2009/NP-TIFR02.

[1] R. Charity, Phys. Rev C **82**, 014610 (2010).
[2] F. Puhlhofer, Nucl. Phys. A **280**, 267 (1977).
[3] L. G. Sobotka, M. L. Padgett, G. J. Wozniak, G. Guarino, A. J. Pacheco, L. G. Moretto, Y. Chan, R. G. Stokstad, I. Tserruya, and S. Wald, Phys. Rev. Lett. **51**, 2187 (1983).
[4] K. Kwiatkowski, J. Bashkin, H. Karwowski, M. Fatyga, and V. E. Viola, Phys. Lett B **171**, 41 (1986).
[5] L. G. Moretto, Nucl. Phys. A **247**, 211 (1975).
[6] L. G. Moretto, K. X. Jing, L. Phair, and G. J. Wozniak, J. Phys. G **23**, 1323 (1997).
[7] K. Jing, Ph.D. thesis, University of California (Berkeley), May 1999 (unpublished).
[8] P. Das *et al.*, Phys. Rev C **66**, 044612 (2002).
[9] A. Ray, P. Das, S. R. Banerjee, A. De, S. Kailas, A. Chatterjee, S. Santra, S. K. Dutta, S. Saha, and S. Roy, Phys. Rev. C **68**, 051602 (2003).
[10] A. Ray, S. Gil, M. Khandaker, D. D. Leach, D. K. Lock, and R. Vandenbosch, Phys. Rev C **31**, 1573 (1985).
[11] B. Shivakumar, S. Ayik, B. A. Harmon, and D. Shapira, Phys. Rev C **35**, 1730 (1987).
[12] D. J. Hinde, D. Hilscher, H. Rossner, B. Gelbauer, M. Lehmann, and M. Wilpert, Phys. Rev C **45**, 1229 (1992).
[13] A. Gavron, A. Gayer, J. Boissevain, H. C. Britt, T. C. Awes, J. R. Beene, B. Cheynis, D. Drain, R. L. Ferguson, F. E. Obenshain, F. Plasil, G. R. Young, G. A. Petitt, and C. Butler, Phys. Rev C **35**, 579 (1987).
[14] P. Paul and M. Thoennessen, Annu. Rev. Nucl. Part. Sci. **44**, 65 (1994).
[15] S. G. McCalla and J. P. Lestone, Phys. Rev. Lett. **101**, 032702 (2008).
[16] J. D. Molitoris, W. E. Meyerhof, Ch. Stoller, R. Anholt, D. W. Spooner, L. G. Moretto, L. G. Sobotka, R. J. McDonald,

G. J. Wozniak, M. A. McMahan, L. Blumenfeld, N. Colonna, M. Nessi, and E. Morenzoni, Phys. Rev. Lett. **70**, 537 (1993).
[17] F. Goldenbaum, M. Morjean, J. Galin, E. Lienard, B. Lott, Y. Perier, M. Chevallier, D. Dauvergne, R. Kirsch, J. C. Poizat, J. Remillieux, C. Cohen, A. L' Hoir, G. Prevot, D. Schmaus, J. Dural, and M. Toulemonde, Phys. Rev. Lett. **82**, 5012 (1999).
[18] J. U. Andersen, J. Chevallier, J. S. Forster, S. A. Karamian, C. R. Vane, J. R. Beene, A. Galindo-Uribarri, J. Gomez del Campo, H. F. Krause, E. Padilla-Rodal, D. Radford, C. Broude, F. Malaguti, and A. Uguzzoni, Phys. Rev. Lett. **99**, 162502 (2007).
[19] V. F. Weisskopf and E. P. Wigner, Z. Phys. **63**, 54 (1930).
[20] L. Fonda, G. C. Ghirardi, and A. Rimini, Rep. Prog. Phys. **41**, 587 (1978).
[21] A. Sudbery, Ann. Phys. (NY) **157**, 512 (1984).
[22] D. Home, *Conceptual Foundation of Quantum Mechanics* (Plenum, New York, 1997).
[23] E. B. Norman, S. B. Gazes, S. G. Crane, and D. A. Bennett, Phys. Rev. Lett. **60**, 2246 (1988).